

Self-Induced Transparency and Resonant Self-Focusing in Atomic Iodine Vapor

J. J. Bannister, H. J. Baker, T. A. King, and W. G. McNaught

Physics Department, Schuster Laboratory, Manchester University, Manchester M13 9PL, England

(Received 17 December 1979)

Self-induced transparency has been observed for the degenerate, $F = 3 \rightarrow 4$, hyperfine component of the $1.315\text{-}\mu\text{m}$ magnetic dipole transition of atomic iodine, at high optical power levels, up to 50 MW cm^{-2} . For pulse areas approaching 2π , the dynamics of the strong coherent resonant self-focusing which accompanies self-induced transparency have been studied with a streak camera to provide time-dependent analysis of the spatial beam profile.

PACS numbers: 42.65.Gv, 42.65.Jx

The interaction of short, intense, coherent optical pulses with resonant nondegenerate and degenerate absorbers leads to the phenomenon of self-induced transparency (SIT), provided that the pulse duration is shorter than the homogeneous relaxation time of the absorbing medium.^{1,2} More recently, self-focusing of on-resonance radiation has been predicted^{3,4} and observed in SIT experiments in sodium vapor and neon.⁵ We report here on the observation of SIT and coherent resonant self-focusing (RSF) for the degenerate magnetic dipole transition ($5^2P_{1/2}, F=3$) \rightarrow ($5^2P_{3/2}, F=4$) of atomic iodine at $1.315\text{ }\mu\text{m}$, using nanosecond-duration, high-energy pulses. Because of the small interaction strength of the magnetic dipole transition the threshold for coherent effects for pulse durations of 100 ps to 1 ns is in the range 30 GW cm^{-2} to 300 MW cm^{-2} . These power levels occur in practicable high-power iodine lasers, and thus coherent phenomena offer a possibility for pulse reshaping.

The atomic iodine laser-absorber combination is self-resonant, with excited-state iodine produced by uv photodissociation of alkyl iodides in the laser, and ground-state iodine produced by thermal dissociation of molecular iodine in the absorber. Of the six possible hyperfine transitions of $5^2P_{1/2} \rightarrow 5^2P_{3/2}$, the $F=3 \rightarrow 4$ has the largest oscillator strength and is produced by a free-running iodine oscillator. The $F=3 \rightarrow 4$ transition is degenerate in zero magnetic field, and gives the dipole distribution shown in Fig. 1 for plane-polarized radiation ($\Delta M_F = 0$). The four values of dipole moment are sufficiently closely grouped to approximate a nondegenerate system with an average dipole moment $\bar{\mu} = 0.37\mu_B$. The magnetic dipole transition requires the pulse area to be defined in terms of the magnetic field envelope,

$$\theta(z, t) = \frac{\bar{\mu}}{\hbar} \int_{-\infty}^t B(z, t') dt'.$$

An energy density of 33 mJ cm^{-2} and a peak power of 19.4 MW cm^{-2} give an area of π for a 1.6-ns full width or half maximum (FWHM) pulse.

The $1.315\text{-}\mu\text{m}$, nanosecond-duration laser pulses are generated by an oscillator-amplifier system, using uv photolysis of $n\text{-C}_3\text{F}_7\text{I}$ by flashlamps to produce population inversion on the atomic iodine transition. The electro-optically mode-locked oscillator⁶ is operated with a 90-Torr $\text{C}_3\text{F}_7\text{I}$ fill; this produces a pulse width of 2 ns, and negligible shift in the oscillation frequency due to pressure-broadened overlap of hyperfine transitions.⁷ Compensation of flashlamp-produced magnetic fields minimizes shifting and splitting of the oscillation frequency, and as a result the laser source matches accurately the line center of the Doppler-broadened $F=3 \rightarrow 4$ transition of low-pressure atomic iodine. The most intense mode-locked pulse from the oscillator is selected by an electro-optic shutter, and amplified by a 16-mm-aperture amplifier operating at 70-Torr $\text{C}_3\text{F}_7\text{I}$ pressure. A partially saturated energy gain of 40 to 50 narrows the oscillator pulse width to 1.6 ns.

The atomic iodine absorption cell, based on the thermal dissociation of molecular iodine vapor, has been described previously.⁸ In the work reported here, a cell temperature of 1000 K and molecular iodine source pressure of 1.5 Torr

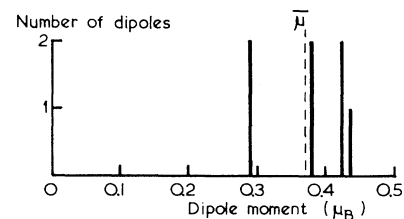


FIG. 1. Magnetic dipole moment distribution for the $F=3 \rightarrow 4$, $\Delta M_F=0$ plane-polarized transition.

gives a small-signal absorption coefficient (αL) of 4 for a beam double passed through the 1.25-m active length by means of a retroreflecting prism. The absorption Doppler linewidth is 460 MHz FWHM, and exceeds the input-pulse spectral width of 275 MHz sufficiently to approximate broad-line SIT conditions.² A beam-contracting telescope is used to produce a closely parallel beam within the cell, of 6 mm diam ($1/e^2$ intensity).

Measurements of pulses transmitted through the cell are made variously with an S1-cathode vacuum photodiode, an S1 photomultiplier, and a germanium photodiode. The vacuum photodiode is highly nonlinear, has a very low and variable sensitivity, and is used only when subnanosecond time resolution is needed. The germanium detector and photomultiplier, with time resolutions of 3 and 7 ns, respectively, are linear and more sensitive and are used for energy transmission measurements. A 1-mm-diam aperture at the output of the cell is used for axial energy density measurements with a calibrated pyroelectric detector and to approximate uniform plane-wave conditions. Time resolution of the output beam profile is obtained with an S1-photocathode streak camera (Hadland-Photonics 675).

An initial aim in this study is to establish characteristic features of SIT, and to rule out incoherent bleaching of the iodine absorber. This has been done by observed transparency, pulse delay, and pulse broadening for pulse areas between π and 2π , in an approximation to uniform plane-wave conditions generated by observing the beam through a 1-mm aperture. Figure 2 shows data obtained with a 1.6-ns-FWHM, Gaussian-shaped input pulse. For small input energies, the absorber shows linear transmission corresponding to $\alpha L = 4$, with slight narrowing of the pulse width [Fig. 2(b)] and a 0.9-ns reduction in the transit time relative to vacuum [Fig. 2(c)]. For a Doppler line shape, the limiting pulse delay for a narrow-band, resonant pulse, calculated from the small-signal velocity, is $t_d = -\alpha L(\ln 2)^{1/2} / \pi^{3/2} \Delta \nu_D = -1.3$ ns.⁹ The observed delay is expected to be of smaller magnitude because the pulse spectral width is comparable to the absorber Doppler width.

Increasing the input energy density above a level of 27 mJ cm^{-2} causes a sharp transition to a region of high transmission, with considerable pulse broadening and delay. To within the energy measurement accuracy of $\pm 20\%$, the transition matches the energy density of 33 mJ cm^{-2} calcu-

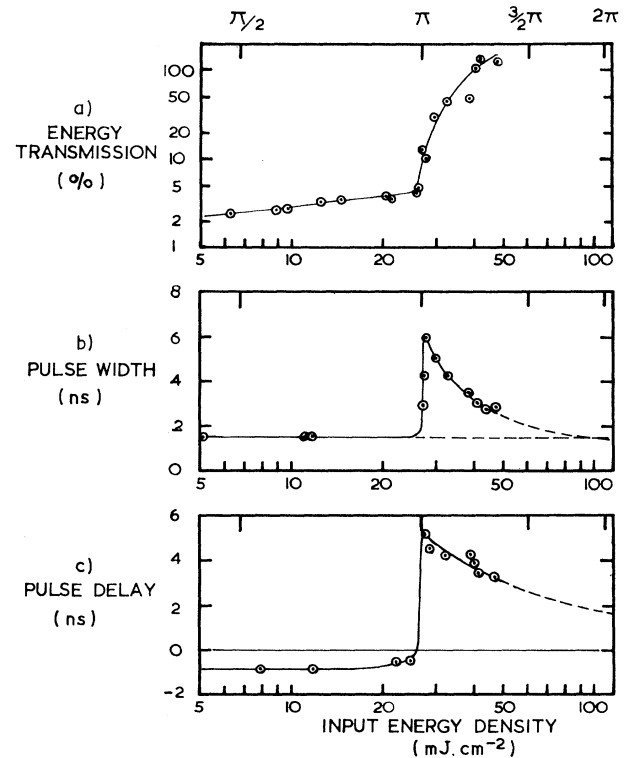


FIG. 2. (a) Energy transmission, (b) pulse width, and (c) pulse delay vs input energy density for a 1.6-ns pulse and $\alpha L = 4$.

lated for a 1.6-ns-duration π pulse, with a mean dipole moment of $0.37\mu_B$. Pulse broadening observed for pulses between π and 2π [Fig. 2(b)] is a characteristic of SIT, and corresponds to evolution towards a 2π hyperbolic secant pulse, where increased width allows the area to increase while the pulse energy is decreasing. The sharp peak in the pulse delay [Fig. 2(c)] at an input area of π has been shown by the numerical calculations of Hopf and Scully¹⁰ to be a feature of SIT which depends strongly on the collisional dephasing time, T_2' , in the medium. Our observation of a very steeply rising delay at π is good evidence that T_2' is considerably greater than the 10-ns time scale of the experiment. While the data presented do not include an area of 2π , the time scale of the delays is consistent with a value of 1.8 ns calculated from the relation $t_d = \frac{1}{2}\alpha L(\tau_p/1.76)$ for a 2π hyperbolic secant pulse,¹¹ with τ_p the FWHM of the intensity pulse.

The agreement of the observed π -pulse energy density with the calculated value and the sensible behavior of the pulse width and delay in the π to 2π region confirms that the high degree of transparency obtained in the iodine system is true

SIT, and not an incoherent bleaching process. A feature of the energy transmission measurements [Fig. 2(a)] is that an effective transmission of 120% has been recorded for the largest input energy, giving evidence that SIT is accompanied by self-focusing in the experiment. The self-focusing discussed here is coherent, on-resonance pulsed self-focusing and should be distinguished from incoherent pulsed or cw self-focusing due to intensity-dependent saturation of the anomalous dispersion.^{12,13}

Self-focusing for coherent on-resonance radiation has been shown to be associated with SIT when the self-focusing parameter, $F = \lambda/4\pi r^2 \alpha$, is in the range 10^{-2} to 10^{-4} and αL is 5 to 30.⁴ In this experiment, $F = 7 \times 10^{-3}$, and resonant self-focusing (RSF) is expected to be important. Previous experimental studies⁵ have observed focusing through changes in the beam energy profile, without being able to study the evolution of focusing within a pulse. To study RSF in iodine, we have used a streak camera, allowing display of the beam profile time dependence.

Figure 3 shows streak recordings of the light transmitted by a 0.1-mm slit aligned across the center of the beam. Simultaneous oscilloscope recordings of the intensity in the whole beam, measured by the 3-ns response time germanium photodiode, are drawn for comparison on a slightly nonlinear time base which matches the streak-camera sweep. With the absorber cell under vacuum [Fig. 3(a)], the streak record confirms the beam diameter of ~ 6 mm and the pulse width of 1.6 ns found by measurements with a phosphor-converter camera and the fast S1 vacuum photodiode. In Fig. 3(b), the input pulse has been adjusted to be slightly in excess of π , on axis. Since transparency occurs only where the area exceeds π , the wings of the profile are stripped off¹ and the beam diameter is reduced to ~ 3 mm. Analysis of photographs at different exposure levels shows that the beam diameter remains approximately constant through the pulse and self-focusing is not detected. Note that in the measurements, a weak second pulse follows the main pulse by 10 ns, as a result of imperfections in the electro-optic pulse selector. The absorber is highly transparent to this second pulse when the first is close to a π pulse, as can be seen in Fig. 3(b).

Increasing the pulse area to $\sim 1.5\pi$ produces the strong progressive focusing shown in Fig. 3(c). The beam diameter decreases with time from ~ 4.2 mm in the leading edge of the pulse, to ~ 1.5

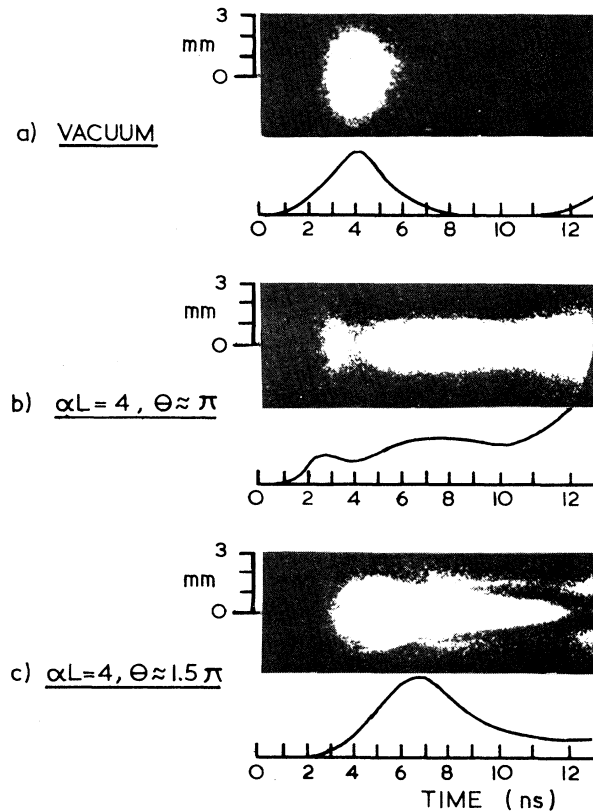


FIG. 3. Streak-camera photographs and corresponding oscilloscope traces for pulses reshaped by SIT. (a) Absorber under vacuum, (b) $\alpha L = 4$, $\theta \approx \pi$, (c) $\alpha L = 4$, $\theta \approx 1.5\pi$.

mm in the trailing edge, with a ring of 3 mm diam being produced after the peak intensity point. Similar diffraction rings have accompanied incoherent self-focusing in K (Ref. 12) and Na (Ref. 14) and may be a general feature of self-focusing irrespective of the physical mechanism responsible for it. The focusing allows the on-axis transparency to exceed 100% in a SIT experiment, and in this case a 120% transparency [Fig. 2(a)] is obtained, while the whole-beam transparency is 70%. The observations are in accord with RSF calculations, which restrict focusing to areas above π , and predict progressive focusing due to build up of radially dependent self-phase modulation in the tail of the pulse, following radially dependent reshaping of the pulse by SIT.⁴

When the input pulse area is near to π , we invariably observe a prepulse, clearly visible in Fig. 3(b). This propagates through the cell with the small-area velocity and attenuation, and is similar to the unexplained prepulse observed by Rhodes and Szöke¹⁵ for SIT in degenerate SF₆.

transitions. The prepulse is not due to small-area propagation of energy in the wings of the beam profile, since the streak photograph shows that the prepulse intensity is strongest on axis. We attribute the presence of a prepulse to the degeneracy of the iodine transition. While five dipoles (Fig. 1) are sufficiently close to see effectively equal pulse areas, the remaining two dipoles at $0.289\mu_B$ require $\sim 70\%$ more energy density to achieve a given area. For energy densities around π , a region exists where the five strongest dipoles respond to an area exceeding π , with transparency and long delay, while the remaining two are below π and respond with essentially the small-area characteristics.

The results presented here are a first demonstration of coherent-pulse propagation phenomena at high powers for an optical magnetic dipole transition. Further work on the degenerate $F = 3 - 4$ transition will involve the use of larger pulse areas where dephasing among the dipole group will become important, and detailed analysis of the dynamics of self-focusing from streak camera records. Longer pulse studies will determine the limits of coherent propagation due to collisional dephasing, while operation on the $F = 2 - 2$ and $F = 3 - 3$ hyperfine transitions using a tunable iodine laser¹⁶ will allow studies of two "ideal" systems of simple degeneracy, with dipole ratios of $1:\frac{1}{2}$ and $1:\frac{2}{3}:\frac{1}{3}$, respectively.

We are pleased to be able to thank Dr. D. R. Gray for his participation in the earlier stages of the experiment. Funding for these experiments

from the Science Research Council is gratefully acknowledged.

¹S. L. McCall and E. L. Hahn, Phys. Rev. **183**, 457 (1969).

²R. E. Slusher, in *Progress in Optics*, edited by E. Wolf (North-Holland, Amsterdam, 1974), Vol. 12, p. 54, and references therein.

³K. Wright and M. C. Newstein, Opt. Commun. **1**, 8 (1973).

⁴F. P. Mattar and M. C. Newstein, IEEE J. Quantum Electron. **13**, 507 (1977).

⁵H. M. Gibbs, B. Bolger, F. P. Mattar, M. C. Newstein, G. Forster, and P. E. Toschek, Phys. Rev. Lett. **37**, 1743 (1976).

⁶H. J. Baker and T. A. King, J. Phys. E **9**, 287 (1976).

⁷E. S. Mukhtar, H. J. Baker, and T. A. King, Opt. Commun. **24**, 167 (1978).

⁸D. R. Gray, H. J. Baker, and T. A. King, J. Phys. D **10**, 169 (1977).

⁹L. Casperson and A. Yariv, Phys. Rev. Lett. **26**, 293 (1971).

¹⁰F. A. Hopf and M. O. Scully, Phys. Rev. B **1**, 50 (1970).

¹¹R. E. Slusher and H. M. Gibbs, Phys. Rev. A **5**, 1634 (1972).

¹²D. Grischkowsky, Phys. Rev. Lett. **24**, 866 (1970).

¹³J. E. Bjorkholm and A. Ashkin, Phys. Rev. Lett. **32**, 129 (1974).

¹⁴A. C. Tam, Phys. Rev. A **19**, 1971 (1979).

¹⁵C. K. Rhodes and A. Szöke, Phys. Rev. **184**, 25 (1969).

¹⁶E. S. Mukhtar, H. J. Baker, and T. A. King, J. Phys. D **11**, 1303 (1978).

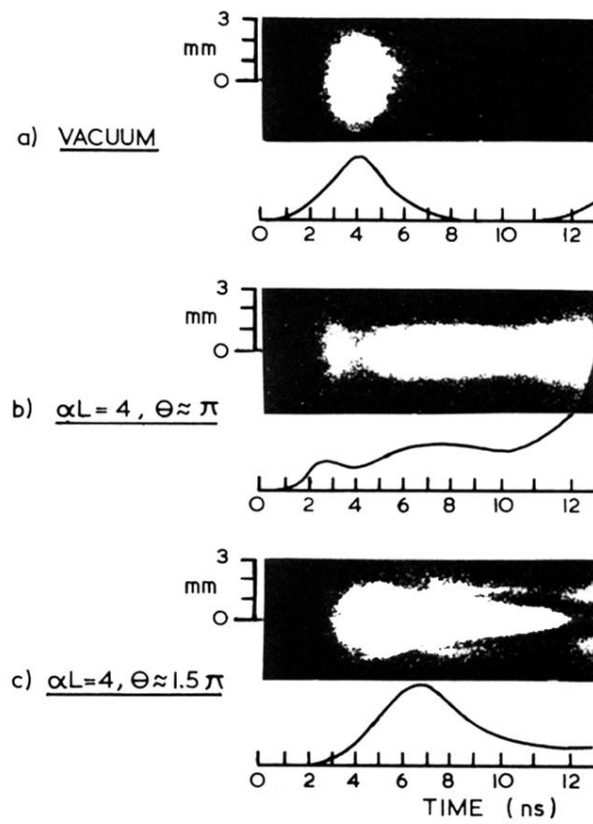


FIG. 3. Streak-camera photographs and corresponding oscilloscope traces for pulses reshaped by SIT. (a) Absorber under vacuum, (b) $\alpha L = 4$, $\theta \approx \pi$, (c) $\alpha L = 4$, $\theta \approx 1.5\pi$.